Contract No.:

This manuscript has been authored by Savannah River Nuclear Solutions (SRNS), LLC under Contract No. DE-AC09-08SR22470 with the U.S. Department of Energy (DOE) Office of Environmental Management (EM).

Non-Aqueous Electrochemical Fluorination of Used Nuclear Fuel as an Advanced Separation Process

Michael J. Martínez-Rodríguez, Luke C. Olson, Joshua R. Gray, and Brenda L. García-Díaz*

Savannah River National Laboratory, Aiken, South Carolina 29808, USA

ABSTRACT

Development of efficient and environmentally benign methods to reprocess used nuclear fuel (UNF) will enable technologies for a nuclear renaissance. Electrochemical and fluorination methods for reprocessing UNF have been proposed, but combinations of electrochemical and fluorination methods have not been investigated. Electrochemical fluorination may reduce waste volumes compared to the main large-scale aqueous methods for processing used nuclear fuel. In this work, a non-aqueous electrochemical fluorination reprocessing method has been developed and demonstrated that enables gas phase uranium recovery while allowing for potential control of the reaction using a single process. Thermodynamic modeling showed a galvanic reaction between UNF and a fluorinating agent, such as NF_3, in a molten fluoride electrolyte was possible and could selectively fluorinate U to UF_6. To verify the model results, a reactor system for electrochemical fluorination was constructed along with vessels for product collection and analysis. Initial trials of the electrochemical reaction were performed and characterized by several electrochemical methods. The electrochemical oxidation of U using NF_3 as an oxidizing agent was demonstrated and UF_6 as a reaction product was detected.

Keywords:

Uranium hexafluoride	Galvanic cell	Fluorinating agents
Potential control	FLiNaK	

Article history:

Manuscript version 4.4
Manuscript submitted to Journal of Electrochemical Society

* *E-mail: brenda.garcia-diaz@srnl.doe.gov*

1. Introduction

One of the main drawbacks to the expansion of nuclear power is the lack of a widely accepted method to process used nuclear fuel (UNF) to separate uranium for reprocessing while minimizing waste and preventing plutonium isolation. UNF processing has simultaneous goals of: 1) separating uranium from fission products (FPs) for reuse, 2) maintaining Pu with other FPs to prevent proliferation, 3) minimizing waste, 4) maximizing separation of waste components, and 5) maximizing process safety. The byproduct (raffinate) of the conventional Plutonium/Uranium Extraction (PUREX) process used to separate fission products for defense purposes is high level waste. The PUREX process can also be used to isolate plutonium. [1] Modifications to the PUREX process have been proposed to reduce waste volumes and prevent plutonium separation [2-4] as well as to isolate individual components. [5-8] But all of the modified PUREX processes would still generate liquid waste streams requiring additional processing.

Alternative non-aqueous separation methods are being developed that do not generate liquid waste and provide benefits for process safety. Two non-aqueous methods that have been developed for nuclear fuel processing are pyroprocessing [9-14] and fluoride volatility. [15-19] Pyroprocessing converts UNF into a metallic form and uses electrorefining in a molten chloride electrolyte to deposit uranium on a stainless steel electrode. The fluoride volatility process fluorinates the elements in UNF by reacting it with fluorine gas at high temperature. The fluorides produced by this reaction segregate between the solid phase and gas phase depending on their boiling point. In this process, uranium hexafluoride is recovered as a gas. Additional separation steps in the fluoride volatility process can further segregate FPs including plutonium. Fluoride volatility separation has also been proposed in a hybrid aqueous separation FLOREX process by Hitachito significantly reduce liquid waste volumes. [20]

Molten fluoride salts have been proposed as the fuel containing component in a Molten Salt Reactor (MSR), and tested in the Molten Salt Reactor Experiment (MSRE) developed at Oak Ridge National Laboratory in the 1960's and 1970's. [21, 22] Fuel processing methods for advanced MSRs have proposed using fluorination to separate UF_6 from other FPs. The possibility of using molten fluorides for UNF pyroprocessing has not been significantly explored and electrochemical fluorination of the UNF to selectively extract UF_6 has not been explored. Fluorine is the most electropositive element and fluorine reduction has an electrochemical reduction potential more than 3 V above the hydrogen electrode and 4-5 V

above the reduction potentials for uranium. This large potential difference should drive fluorine to oxidize uranium in a galvanic electrochemical reaction with high kinetics. In addition to fluorine, other fluorinating agents such as NF_3, SF_6, or XeF_2 could also be used to electrochemically oxidize the UNF. The electrode potentials can be controlled using a load that applies a specific resistance. Potential control could be used to fluorinate only the uranium in the UNF and ensure that UF_6 is produced. Potential control could also be used to ensure plutonium is oxidized to PuF_4 without production of gaseous PuF_6.

Electrochemical fluorination is proposed to separate uranium from other fission products by electrochemistry to precisely control reaction products and rates. [23, 24] Separation of UNF components using electrochemical fluorination incorporates aspects of current electrorefining and fluoride volatility processes. An example diagram of an UNF process is shown in Figure 1. The electrochemical fluorination method is used to reduce or eliminate gas phase rectification of products from fluoride volatility methods since only UF_6 would be rendered gaseous. Plutonium fluorides will remain in solution for collection in a liquid cadmium cathode. Uranium depositon and extraction operaitons as used in molten chloride methods would not be required. The objective of this work is to demonstrate the thermodynamic feasibility of electrochemical fluorination for UNF separations and demonstrate the electrochemical fluorination of uranium.

2. Thermodynamic Calculations

Reprocessing UNF in molten fluorides requires understanding how the thermodynamics and ions in the electrolyte are affected by electrochemical potential and other mixture components. This section outlines the calculations and analysis that provide the thermodynamic basis for the process.

2.1. Thermodynamic Foundation

The equilibrium cell potential (E) of an overall reaction to be carried out electrochemically is calculated from the Gibbs free energy (ΔG) of reaction according to the equation:

$$E = \frac{-\Delta G}{nF} \tag{1}$$

where n is the number of electrons transferred in the reaction and F is Faraday's constant.

The Gibbs free energy for the reaction is calculated from free energy of formation (ΔG_f)data by

$$\Delta G = \sum_i s_i \Delta G_{i,f} \tag{2}$$

where s_i is the stoichiometric coefficient for species i (positive for products and negative for reactants). The electrode potential can be obtained using Eq. (1) and (2) when the quantities refer to the reversible redox reaction occurring at the electrode. At standard conditions (25°C and unit activity for the species) the equilibrium electrode (or cell) potential is expressed as

$$E^o = \frac{-\Delta G^o}{nF} \tag{3}$$

The following equation corrects for temperature:

$$\left(\frac{\partial E}{\partial T}\right)_P = \frac{\Delta S}{nF} \tag{4}$$

where T is temperature, P indicates constant pressure and (ΔS) is the entropy of the reaction. For a temperature range where ΔS can be considered constant Eq. (4) yields

$$E_{T_2} = E_{T_1} + \frac{\Delta S}{nF}(T_2 - T_1) \tag{5}$$

The software HSC Chemistry 7 contains a thermochemical database that was used in calculations of the electrode (or cell) potentials at the required temperature. The electrochemical calculations were performed for most FPs using the general equation:

$$MF_n + ne^- \leftrightarrow M + nF^- \tag{6}$$

where:

M is a fission product

In HSC, the electrode reactions were written as a reduction so that the potentials calculated are reduction potentials. The equilibrium potentials were referenced against the hydrogen electrode (H_2/H^+). In molten fluorides, it is more practical to use a Ni/NiF_2 reference. The equation below was used to convert the potential reference from hydrogen to Ni

$$E^{T}_{M,Ni} = E^{T}_{M,H_2} - E^{T}_{Ni,H_2} \quad (7)$$

where:

$E^{T}_{M,Ni}$ is the equilibrium potential of FP M at temperature T with respect to a Ni/NiF_2 reference at T

E^{T}_{M,H_2} is the equilibrium potential of FP M at temperature T with respect to a H_2/H^+ reference at T

E^{T}_{Ni,H_2} is the equilibrium potential of Ni/NiF_2 at temperature T with respect to a H_2/H^+ reference at T

2.2. Analysis

Thermodynamic calculations of half-cell potentials for possible electrochemical reactions for UNF constituents were performed in HSC Chemistry 7. The potentials were normalized against a Ni/NiF_2 reference. Thermodynamic analysis was conducted at temperatures between 0°C and 800°C.

The first set of calculations illustrate the feasibility of fluorinating the spent nuclear fuel elements and also show that volatile UF_6 can be produced with minimal production of other volatile fluorides. Figure 2 contains the results of electrode potential calculations for fluorinating agents such as F_2, NF_3, and XeF_2 as well as major gaseous fission products.

The equilibrium potentials for the fluorinating agents are approximately 1.5 V higher than equilibrium potentials for creation of volatile fluorides. In this diagram, higher potentials indicate greater ability for the chemical to act as an oxidizing agent. Since the oxidizing agent has a more positive potential than the oxidant, the volatilization of fission products would be galvanic and happen spontaneously. The higher potentials for the fluorinating agents indicate that all of the FPs listed would be rendered volatile upon reaction with any of the fluorinating agents in a short-circuited cell with minimal electrolyte resistance. However, when potential control is used in a galvanic cell, the FPs with more negative equilibrium potentials can be selected for preferential oxidation before FPs. Certain reactions may be kinetically or mass transfer limited and thus result in low or negligible reaction rates.

Figure 2 also shows that the potential difference between the equilibrium for formation of UF_6 and NpF_6 is approximately 400 mV. Therefore, even with substantial overpotential,

uranium metal could be electrochemically oxidized to UF_6 before NpF_6 could be produced. It is less likely that PuF_6, which is about 700 mV above the equilibrium, would be produced. The potential of the spent nuclear fuel could be below the nickel fluorination potenential. The equilibrium potential for nickel is important since it is one of the primary materials used in construction of the reaction vessel. In ORNL report 4574 [15] on the fluoride volatility process for the molten salt reactor, they note that the only volatile fluoride FPs that could not be easily extracted by passing the gas through a NaF bed were TcF_6, TeF_6, and MoF_6. None of these fluorides should be formed using electrochemical fluorination since the potential of the spent nuclear fuel would be controlled well below those values.

The equilibrium potentials for the transuranic (TRU) or minor actinide (MA) elements are given in Figure 3. The potentials in this figure represent the equilibria between the metallic spent fuel elements and the dissolved salt constituents. All the TRU salt constituents could be deposited out of solution after volatilization of the uranium by reducing the potential of an electrowinning electrode below around -2.10 V vs. Ni/NiF_2 at 500°C.

The reduction potentials for alkaline metals (AMs), alkaline earth metals (AEMs), and lanthanides (Ln's) are shown in Figure 4. The alkali metals had the highest reduction potentials followed by the lanthanides and Y, which has many similar properties to the Ln's. The lowest reduciton potentials were for AEMs.

An additional set of calculations for other possible primary salt were performed and plotted over the data in Figure 4. The plot of the equilibrium potentials of salt constituents is shown in Figure 5. It can be seen that if it is desired to separate the lanthanides by electrowinning from the solvent, then only LiF and CaF_2 could be used since NaF, KF, BeF_2, and MgF_2 would start depositing out of the solution before the lanthanides. LiF-NaF-KF (FLiNaK) would still likely be the best solvent to attempt electrochemical fluorination because of its fluorobasicity (ability to donate fluoride ions). Bieber et al. [25] showed that the binary mixtures of NaF-KF and LiF-KF had the highest fluorobasicity of all common molten fluoride solvent mixtures.

3. Experimental

An electrochemical fluorination process and separation system was developed capable of separating gas phase uranium through electrochemical potential control of the reaction. The reaction was carried out in a molten fluoride eutectic salt mixture. The salt that has been the

focus of this work is the eutectic LiF–NaF–KF (46.5, 11.5, and 52 mol%, also known as FLiNaK) due to its high basicity, low melting point (727 K), and commercial availability. FLiNaK was obtained from Electrochemical Systems, Inc., which was prepared as described in the experimental section of Olson et al. [26] and detailed in Holcomb and Cetiner. [27] NF_3 (99.5% Air Liquide) was used as the fluorinating agent and depleted uranium (DU) was used as a surrogate material for used nuclear fuel (UNF). DU metal turnings were degreased with anhydrous ethanol and the black oxide layer removed with an 8 M nitric acid solution.

3.1. Electrochemical Reactor and Setup

A custom electrochemical reactor and electrodes were fabricated for the electrochemical fluorination as shown in Figure 6. The electrochemical reactor consisted of a stainless steel vessel of approximately 15 cm diameter used as the embodiment for the electrochemical cell and the feed through for gases, thermocouple and electrodes. Inside the vessel, a secondary non-conducting ceramic container held a glassy carbon crucible which contained the FLiNaK (electrolyte). The cathode was a gas diffusion electrode that used a glassy carbon tube with a porous reticulated vitreous carbon frit at the bottom to diffuse the NF_3 gas. The glassy carbon tube was inserted through a larger quartz tube to electrically isolate the cathode from the main vessel. The anode consisted of a fused quartz tube with a center Ni wire and a graphite or Ni basket at the bottom to hold the DU as shown in Figure 7. The Ni wire was maintained in electrical contact with the DU turnings while holes drilled through the graphite or Ni allowed contact of the DU with FLiNaK. The reference electrode was fabricated similar to Kontoyannis. [28] It consisted of a fused quartz tube with a center Ni wire and graphite basket at the bottom holding 1 mol% Ni/NiF_2 in FLiNaK.

The electrochemical cell assembly and reactor loading were performed in a glove bag using nitrogen. The glove bag provided an inert atmosphere to preserve the purity of FLiNaK, the salt mixture for the reference electrode and the depleted uranium. The reactor was sealed and then transferred to a chemical hood, where the gas manifold was located, and set in a furnace. The electrodes from the electrochemical cell that come out through the top of the reactor were connected to a Bio-Logic potentiostat VSP with a 2 A current booster VMP3 to control the electrochemical reaction, and the reactor was connected to the potentiostat ground to act as a faraday cage to reject electromagnetic noise from the heater. The reactor interfaced with the gas manifold system through two inlets: N_2 and NF_3 (cathode) and one outlet.

3.2. Electrochemical Fluorination System and Operation

The electrochemical fluorination system (EFS) consisted of a gas manifold, the reactor vessel, two stainless steel vessels (about 7.6 cm diameter and 30.5 cm in height) used as cold traps to desublime UF_6, a stainless steel vessel that traped excess NF_3, and a custom sample tube (about 2.5 cm diameter and 10.2 cm in height) that collected UF_6 for analysis. The cold traps contained a baffle assembly and were cooled using a mixture of ethanol and dry ice. The chemical trap was packed with BASF F-200 activated alumina. Gas cylinders for N_2 and NF_3 were connected to the inlet of the system while vacuum was connected to the outlet. Figure 8 shows a flow diagram of the system. All vessels in the system were cleaned with DI water and degreased and dried with ethanol. All Swagelok components were SC-11 cleaned

The gas manifold (enclosure in dotted lines in Figure 8) was designed to simultaneously control the path and flow of gases and vacuum. It was built using the Swagelok integrated gas components II (IGC II) which resulted in a miniature modular system that allowed its assembly in a single chemical hood. This system was equipped with two MKS mass flow controllers (MFC), an MKS pressure controller (PC) and state-of-the-art hardware coupled with LabView programing to control mass flow, temperature and pressure. During a typical experiment, the EFS was first operated to perform the electrochemical fluorination (*reaction mode*) followed by a second procedure for the sample collection (*analysis preparation mode*).

Before starting the experiment, several evacuation cycles and N_2 purge cycles are performed with all equipment attached to the system. The system ended fully evacuated and the valves to the sample collection tube (SCT) were closed. The reactor was heated to 300°C with 100 kPa and a flow of 50 sccm of N_2. At 300°C, the reactor was evacuated for at least 1 hour to remove residual moisture, while heating to a final temperature of 550°C was continued. When the system reached 550°C a path was opened to flow N_2 through the reactor and cold traps through both MFCs. The flow was set to 28 sccm in the N_2 MFC and to 6.96 sccm in the "NF_3" MFC. Note that the latter was N_2 flowing at 6.96 sccm through the "NF_3" MFC. The total system pressure was set to 50 kPa and the system was allowed to approach steady state.

In *reaction mode*, Figure 9(a), the vessel was operated at 550°C and under partial vacuum by controlling the total pressure to 50 kPa. The vessel contained the FLiNaK salt and about 3 g of DU in the anode with 6.96 sccm NF_3 flowing through the cathode. N_2 cover gas flowed at 28 sccm directly through the head space of the vessel to sweep out reaction products, and

vacuum pressure was controlled to maintain a partial pressure of UF_6 below the desublimation pressure, including parts of the gas manifold at room temperature. As the reaction proceeded, the NF_3 was electrochemically reduced and the DU was electrochemically oxidized as shown in the following galvanic reactions:

Anode: $$U_{(s)} + 6F^- \rightarrow UF_{6(g)} + 6e^- \quad (8)$$

Cathode $$2NF_{3(g)} + 6e^- \rightarrow 6F^- + N_{2(g)} \quad (9)$$

Overall $$U_{(s)} + 2NF_{3(g)} \rightarrow UF_{6(g)} + N_{2(g)} \quad (10)$$

The only volatile actinide fluoride was UF_6 which was drawn off to desublime in the cold trap.

Once the reaction was complete, the flow of gases was stopped and the reactor was isolated from the gas manifold. The pressure controller was adjusted to allow close to full vacuum to the cold trap to remove N_2 and excess NF_3, leaving only the solid UF_6. The cold trap was then closed to isolate the solid UF_6,. The cold trap was then warmed to room temperature. Once the system was steady, UF_6 gas would have reached equilibrium with the solid phase and the system was ready to be operated in *analysis preparation mode*.

In *analysis preparation mode*, Figure 9(b), only the cold trap with UF_6 in equilibrium and the SCT with the gas manifold interconnections were used. The UF_6 was transferred from the cold trap (at room temperature) to the collection tube. For this process, the collection tube was evacuated and cooled with a mixture of ethanol and dry ice while the cold trap was maintained at room temperature. A pressure transducer was used in the gas manifold interconnections to monitor the pressure during the UF_6 transfer. Once the collection tube was evacuated and the gas manifold interconnections were isolated from the rest of the system, the valve of the cold trap was opened to allow UF_6 transfer to the collection tube. This process was monitored until the pressure reached equilibrium.

3.3. Characterization

Electrochemical characterization techniques were performed in the molten salt with an N_2 covergas and with NF_3 flow. The open circuit voltage (OCV) was measured with the system at 550°C and 50 kPa, and N_2 flowing through both MFCs. The OCV was run with the DU electrode as the working electrode and the glassy carbon electrode (N_2 bubbling) as the counter. An electrochemical impedance spectroscopy (EIS) measurement was performed at

these conditions to characterize the electrolyte conductivity. The impedance spectrum was obtained in single-sine mode around OCV with a sinus amplitude of 20 mV. The sweeping frequencies were over the 200 mHz – 200 kHz range, recording 6 points per decade and averaging 10 measurements per frequency. Following the EIS, cyclic voltammetry (CV) was performed on the DU electrode to characterize the reactions under the inert environment. The potential was swept between 0 V and -2.25 V vs Ni/NiF_2 at a scan rate of 100 mV/s. Measurements were performed over the last 50% of the step duration, recorded, and averaged over 10 voltage steps. The potentials were allowed to return to steady state after the CV, and were followed by a zero-resistance ammeter (ZRA) experiment. The ZRA was run between the glassy carbon electrode and the DU electrode. This was used as the baseline for the ZRA measurements with NF_3.

A second set of electrochemical tests were performed with NF_3 flowing through the porous glassy carbon electrode. Starting from OCV, and once the system returned to steady state, the flow of NF_3 was set to 6.96 sccm. Once a jump was observed in the counter electrode potential, the flow rate of NF_3 was set to 0 sccm and a ZRA experiment was started. This purged the NF_3 gas from the porous electrodewith N_2. The ZRA experiment was run with no NF_3 flow for 5 minutes. Then, the NF_3 flow rate was increased to 1.16 sccm for 5 minutes. The flow rate was then sequentially increased every 5 minutes, from 1.66 sccm to 2.32, 4.64, 6.96, and 13.92 sccm, respectively, and was finally set back to 0 sccm at the 30 minute mark. The cell was returned to OCV with no NF_3 flow until the system returned to steady state. The flow of NF_3 was set to 6.96 sccm and once a jump was observed in the counter electrode potential a linear sweep voltammetry (LSV) was started. The LSV was performed by scanning the voltage from OCV to 0 V vs Ni/NiF_2 at a scan rate of 10 mV/s. Measurements were performed over the last 50% of the step duration and recorded and averaged over 10 voltage steps. This LSV experiment performed a polarization scan on the DU electrode to see all possible reactions in the system with the NF_3 counter electrode. Finally, a chronoampeometry experiment was used to perform the electrolysis to generate UF_6. The voltage of the DU working electrode was adjusted to 1.5 V vs Ni/NiF_2 and the electrolysis was run for 4 - 5 hrs.

After the electrolysis was completed, the EFS was setup for the *analysis preparation mode* as described previously. The UF_6 in the SCT, Figure 9(c), was processed according to ASTM C1346-08 practices [29] and immersed in water for dissolution as shown on Figure 9(d). The UF_6

was hydrolyzed according to the following reaction

$$UF_{6(s)} + 2H_2O_{(l)} \rightarrow UO_2F_{2(aq)} + 4HF_{(aq)} \quad (11)$$

The presence of U from UO_2F_2 was determined by inductively coupled plasma mass spectrometry (ICP-MS).

4. Results and Discussion

An EFS was designed and fabricated to test the feasibility of the electrochemical fluorination reaction of U to UF_6. Thermodynamic calculations showed that when a fluorinating agent, such as NF_3, was used, the process was galvanic as described by reactions (8) to (10). This process was accomplished by controlling the potential of the U oxidation reaction in a molten fluoride salt mixture (electrolyte). Figure 10 shows the Nyquist plot for the EIS measurement performed after the system reached steady state at 550°C and 50 kPa under an inert environment. The EIS was used to provide an estimate of the electrolyte conductivity (or resistance) using the designed electrodes. The high frequency intercept corresponded to the ohmic resistance value of the circuit (electrolyte, electrodes, instrument, wires and connections) which was dominated by the electrolyte. This resistance was less than 1 ohm and, for the electrodes that were about 3 cm apart, it demonstrated that larger cells could be constructed with minimal loss of efficiency.

Before performing the electrochemical fluorination, a CV was used to characterize the uranium electrode reactions under the inert environment. Figure 11 shows two cycles of the CVs carried out at the same temperature and partial vacuum conditions described above. The two cycles were shifted by about 7 mV and showedsimiliar distinct oxidation and subtle reduction peaks. The CVs exhibited oxidation peaks in the anodic sweep at -0.36 V and -0.30 V vs Ni/NiF_2 for each respective cycle with a reduction peaks in the cathodic sweep at -0.72 V and -0.65 V vs Ni/NiF_2. These peaks were in the range of potentials for U oxidation to UF_3 or UF_4 complexes in the molten salt [30]. The smaller reduction peaks likely correspond to the reduction reactions of uranium fluoride complexes formed during the anodic sweep. The oxidation and reduction of U was reversible as has previously been observed. [30]

In order to capture as much of the reaction as possible, the electrochemical experiment was ran as a ZRA while the flow rate of NF_3 was slowly increased in a stepwise fashion, from zero to 1.5 times the stoichiometric amount. Figure 12 shows the current and electrode potential

response as the NF_3 flow was increased. The maximum reaction occurred at a flow that stoichiometrically would gve a current of 250 mA, but the maximum current observed was 95 mA. Increasing the flow further decreased the reaction rate. This counter intuitive result can be explained due to the NF_3 reduction electrode needing good three-phase contact (electrolyte, gas, electrode), and it was likely that above the 95 mA value, not enough electrolyte was able to stay in the pores. Subsequent increased NF_3 flow created more turbulence in the electrode, due to the gas bubbling, resulting in the decrease of the current and the noisy readings. Increased system pressure with constant NF_3 partial pressure allowed currents up to 7 times as large in subsequent experiments. These results indicated mass transfer limitations which would require optimizing the porous electrode. However, an encouraging sign was the oxidation potential of the electrode which reached up to 1.5 V vs Ni/NiF_2. The reduction of NF_3 occurs at potentials below 2.5 V (a very high value). The 1.5 V voltage observed was also significantly higher than the UF_6 equilibrium potential of -0.55 V vs Ni/NiF_2 that was calculated in Figure 3. This indicated that the formation of UF_6 can occur spontaneously. The 2.5 V equilbrium potential was much higher than the degradation potential for the glassy carbon electrode being used. The glassy carbon was likely cathodically protected by the uranium, but this meant the electrode was relatively stable under these conditions. No signs of the glassy carbon electrode degrading were observed.

A LSV polarization curve for the electrochemical fluorination was obtained with NF_3 flowing at 6.96 sccm. Figure 13 shows that the polarization curve followed the Tafel equation well up to 100 mV of overpotential. The linear form of the Tafel equation can describe the overpotential (η) as function of the current density (i) for the anodic reaction as follows:

$$\eta = a + b\log(i) \tag{12}$$

where the Tafel constants are

$$a = -\frac{2.303RT}{\alpha nF}\log(i_o) \tag{13}$$

$$b = \frac{2.303RT}{\alpha nF} \tag{14}$$

On the equations above, α is the electron transfer coefficient, i_o is the exchange current density and R is the gas constant. From Figure 13 the exchange current density for this reaction

was relatively high at 0.45 mA and the kinetics were fast since the current increased by approximately 10 times for every 160 mV increase in voltage. Mass transfer limitations appeared at overpotentials above 200 mV. A better electrode design would likely help to improve the current and reaction rate.

After the electrochemical characterization of the reaction was completed, electrolysis was performed for about 5 hrs by controlling the DU working electrode to 1.5 V vs Ni/NiF_2. During this part of the process, described as the *reaction mode* and shown in Figure 9(a), the temperature of the reactor was maintained at 550°C and the pressure of the EFS, including the reactor, at 50 kPa. The flow of N_2 through the reactor was adjusted to 28 sccm while the flow of NF_3 through the gas diffusion cathode was adjusted to 6.96 sccm, such that the flow ratio of N_2:NF_3 was kept at 4:1. The flow of 6.96 sccm of NF_3 was stoichiometric for 1.5 A. According to reaction (10) and assuming all NF_3 reacts, UF_6 would be produced at a rate of 3.48 sccm with 3.48 sccm N_2. At these conditions, the partial pressure of UF_6 would be 5 kPa. At 550°C and 5 kPa, the phase diagram in Figure 14 shows that UF_6 is in gas phase (location A). The products of the reaction, any unreacted NF_3 and the N_2 exited the reactor and passed through the gas manifold and cold trap. The gas manifold was at room temperature but still under partial vacuum; consequently UF_6 was in gas phase in this part of the system (location B). However, as UF_6 entered the cold trap, where the temperature drops to -78°C, the phase diagram indicates it will desublime (location C). Baffles in the cold trap provided more contact area for desublimation, while excess NF_3 and N_2 passed through the cold trap. Any excess NF_3 would be captured in the chemical trap.

After the electrolysis was completed the EFS was setup for *analysis preparation mode* as described in the experimental section. The process of applying vacuum to remove N_2 from the cold trap was performed quickly (within 1 min) to minimize loss of UF_6 which can exist in gas phase due to a finite vapor pressure. Once the cold trap was isolated from the gas manifold, it was allowed to warm. After reaching room temperature, the content of the cold trap is mostly UF_6 in gas phase and at about 3 kPa (see location D in Figure 14) in equilibrium with any remaining solid phase. During the transfer of UF_6 to the SCT, the temperature at the SCT was -78°C or less (initially under vacuum), while the cold trap was at room temperature as shown in Figure 9(b). UF_6 gas moved from the cold trap to the SCT due to pressure difference and desublimed at the SCT due to the temperature drop (location E in Figure 14). The pressure

difference was created by the removal of UF_6 from the gas phase to the solid phase in the SCT. This kept the pressure gradient between the cold trap and the SCT, and hence the transport of UF_6 to the SCT. This process was continued until an equilibrium was reached. This condition consisted of UF_6 gas in equilibrium with the solid phase in the cold trap and SCT. At this point the SCT was isolated and disconnected from the gas manifold for analysis of U. After processing the SCT, according to ASTM C1346-08 practices, [29] the amount of U-238 detected by ICP-MS was 1.5 ppt, indicating that UF_6 was produced. This amount corresponds to the U-238 from the UF_6 transferred until equilibrium and does not account for all the UF_6 produced from the electrolysis. Some UF_6 may have been lost during the application of vacuum to remove N_2 from the cold trap while the other portion was the one retained in the cold trap as part of the equilibrium condition during the transfer to the SCT.

5. Conclusions

Thermodynamic calculations were performed for common constituents of SNF and it was shown that it was likely that UF_6 could be separated from the mixture without volatilizing other SNF components. It was shown that other TRU components would remain in the salt after reaction of U and that the TRU elements including Pu could be electrowon from solution at a potential of around -2.10 V vs Ni/NiF_2. Electrowinning at this potential would leave the AMs, Ln's, and AEMs dissolved in solution. The ability to electrowin the Ln's from solution would depend on the stability of the reduction potential of the salt at the reaction temperature.

A custom EFS, which included a compact gas manifold, traps, sample collection and reactor vessels, coupled with state-of-the-art hardware, was designed and fabricated. The system could operate the reactor with variable gas composition and pressure, while allowing recovery of the UF_6 product. Electrochemical characterization demonstrated the ability to electrochemically oxidize uranium using NF_3 as an oxidizing agent. While the amount of UF_6 collected was small, the product analysis showed the presence of UF_6. It was believed the low amount of UF_6 collected was due to lack of optimized experimental procedures. Future experiments and system characterization will be focused on quantifying and improving the process efficiency and yield. This system presented a viable new method for nuclear fuel reprocessing and the development of a processing scheme that could start with oxide UNF.

Acknowledgements

Financial support for this work was provided by the Laboratory Directed Research and Development (LDRD) program. Savannah River National Laboratory is operated by Savannah River Nuclear Solutions. The authors acknowledge Greggory D. Creech, Donald L. Fisher, Henry T. Sessions, Jr., Damon Click, Scott D. Greenway, and José M. Pérez-Berríos for their technical assistance on the setup and various components design of the EFS.

References

1. J. M. McKibben, *Radiochimica Acta*, **36**, 3 (1984).
2. M. C. Regalbuto, in *Advanced Separation Techniques for Nuclear Fuel Reprocessing and Radioactive Waste Treatment*, K. L. Nash and G. J. Lumetta Editors, p. 176, Woodhead Publishing (2011).
3. M. C. Thompson, M. A. Norato, G. F. Kessinger, R. A. Pierce, T. S. Rudisill and J. D. Johnson, Demonstration of the UREX Solvent Extraction Process with Dresden Reactor Fuel Solution, WSRC-TR-2002-00444, Westinghouse Savannah River Company, Aiken, SC (2002).
4. M. C. Thompson, M. A. Norato, G. F. Kessinger, R. A. Pierce, T. S. Rudisill and J. D. Johnson, Demonstration of the UREX Solvent Extraction Process with Dresden Reactor Fuel, WSRC-MS-2003-00089, Rev 1, Westinghouse Savannah River Company, Aiken, SC (2003).
5. K. L. Nash, *Solvent Extraction and Ion Exchange*, **33**, 1 (2015).
6. M. P. Jensen, R. Chiarizia, J. S. Ulicki, B. D. Spindler, D. J. Murphy, M. M. Hossain, A. Roca-Sabio, A. de Blas and T. Rodríguez-Blas, *Solvent Extraction and Ion Exchange*, **33**, 329 (2015).
7. J. N. Mathur, M. S. Murali and K. L. Nash, *Solvent Extraction and Ion Exchange*, **19**, 357 (2001).
8. E. Philip Horwitz, D. C. Kalina, H. Diamond, G. F. Vandegrift and W. W. Schulz, *Solvent Extraction and Ion Exchange*, **3**, 75 (1985).
9. T. Hijikata and T. Koyama, *Journal of Engineering for Gas Turbines and Power-Transactions of the Asme*, **131** (2009).
10. T. Koyama, T. Hijikata, T. Usami, T. Inoue, S. Kitawaki, T. Shinozaki, M. Fukushima and M. Myochin, *J. Nucl. Sci. Technol.*, **44**, 382 (2007).
11. T. Koyama, M. Iizuka, Y. Shoji, R. Fujita, H. Tanaka, T. Kobayashi and M. Tokiwai, *J. Nucl. Sci. Technol.*, **34**, 384 (1997).
12. C. C. McPheeters, E. C. Gay, E. J. Karell and J. P. Ackerman, *Jom-Journal of the Minerals Metals & Materials Society*, **49**, 22 (1997).
13. T. Nishimura, T. Koyama, M. Iizuka and H. Tanaka, *Progress in Nuclear Energy*, **32**, 381 (1998).
14. Z. Tomczuk, J. P. Ackerman, R. D. Wolson and W. E. Miller, *Journal of the Electrochemical Society*, **139**, 3523 (1992).
15. W. H. Carr, L. J. King, F. G. Kitts, W. T. McDuffee and F. W. Miles, Molten-Salt Fluoride Volatility Pilot Plant: Recovery of Enriched Uranium from Aluminum-Clad Fuel Elements, ORNL-4574, Oak Ridge National Laboratory, Oak Ridge, TN (1971).
16. J. Gray, P. Korinko, B. Garcia-Diaz, A. Visser and T. Adams, Reactive Gas Recycle for Used Nuclear Fuel, FCRD-SEPA-2010-000177, Savannah River National Laboratory, Aiken, SC (2010).
17. R. Scheele, B. McNamara, A. M. Casella and A. Kozelisky, *Journal of Nuclear Materials*, **424**, 224 (2012).
18. R. D. Scheele, A. M. Casella and B. K. McNamara, *Industrial & Engineering Chemistry Research*, **56**, 5505 (2017).
19. J. Uhlir and M. Marecek, *Journal of Fluorine Chemistry*, **130**, 89 (2009).
20. H. Kobayashi, O. Amano, F. Kawamura, M. Aoi, K. Hoshino, A. Sasahira and Y. Kani, *Prog. Nucl. Energy*, **47**, 380 (2005).

21. J. Serp, M. Allibert, O. Beneš, S. Delpech, O. Feynberg, V. Ghetta, D. Heuer, D. Holcomb, V. Ignatiev, J. L. Kloosterman, L. Luzzi, E. Merle-Lucotte, J. Uhlíř, R. Yoshioka and D. Zhimin, *Prog. Nucl. Energy*, **77**, 308 (2014).
22. D. LeBlanc, *Nucl. Eng. Des.*, **240**, 1644 (2010).
23. B. L. García-Díaz, M. J. Martínez-Rodríguez, J. R. Gray and L. C. Olson, U.S. Patent 9,382,632 B2, (2016).
24. B. L. García-Díaz, M. J. Martínez-Rodríguez, J. R. Gray and L. C. Olson, U.S. Patent 9,562,297 B2, (2017).
25. A. L. Bieber, L. Massot, M. Gibilaro, L. Cassayre, P. Chamelot and P. Taxil, *Electrochimica Acta*, **56**, 5022 (2011).
26. L. C. Olson, R. E. Fuentes, M. J. Martinez-Rodriguez, J. W. Ambrosek, K. Sridharan, M. H. Anderson, B. L. Garcia-Diaz, J. Gray and T. R. Allen, *Journal of Solar Energy Engineering*, **137**, 061007 (2015).
27. D. E. Holcomb and S. M. Cetiner, An Overview of Liquid-Fluoride-Salt Heat Transport Systems, ORNL/TM-2010/156, Oak Ridge National Laboratory, Oak Ridge, TN (2010).
28. H. Wang, N. J. Siambun, L. P. Yu and G. Z. Chen, *Journal of the Electrochemical Society*, **159**, H740 (2012).
29. A. International, Standard Practice for Dissolution of UF6 from P-10 Tubes, in, West Conshohocken, PA (2014).
30. C. Hamel, P. Chamelot, A. Laplace, E. Walle, O. Dugne and P. Taxil, *Electrochimica Acta*, **52**, 3995 (2007).
31. Office of Nuclear Energy Science and Technology, Final Programmatic Environmental Impact Statement for Alternative Strategies for the Long-Term Management and Use of Depleted Uranium Hexafluoride, DOE/EIS-0269, U.S. Department of Energy, Washington, DC (1999).

List of Figures

Figures

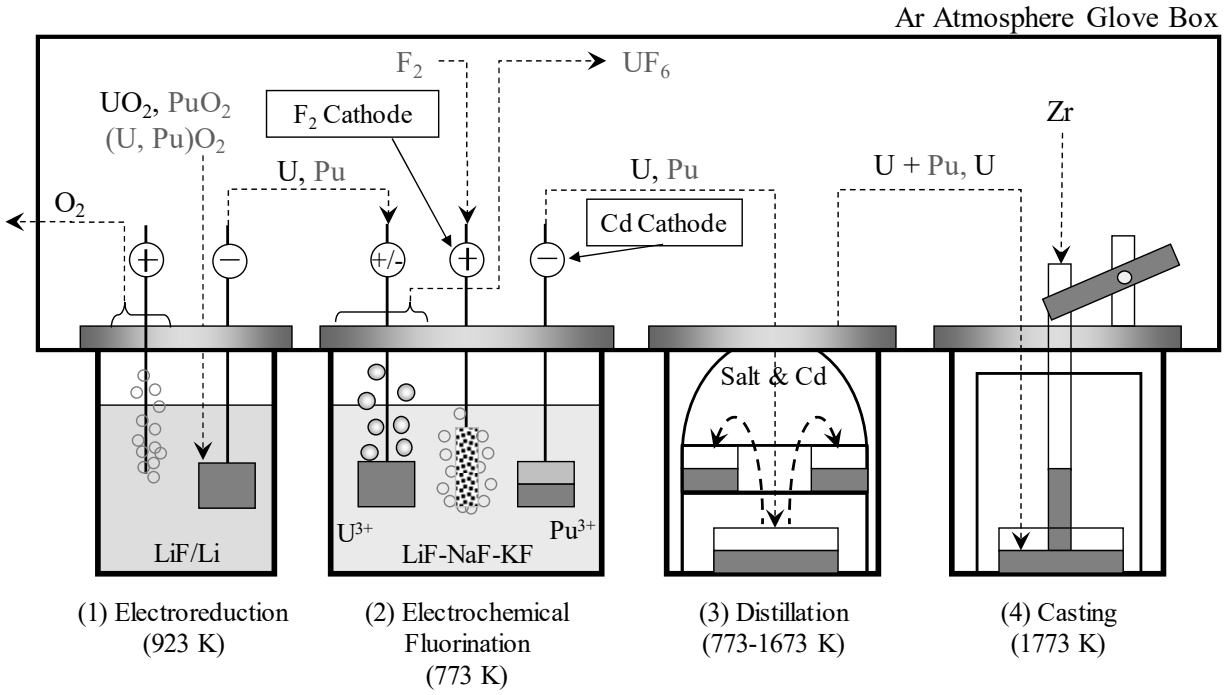

Figure 1: Proposed electrochemical fluorination and extraction process (adapted from Koyama et al.[10] to show the electrochemical fluorination incorporated with other processes).

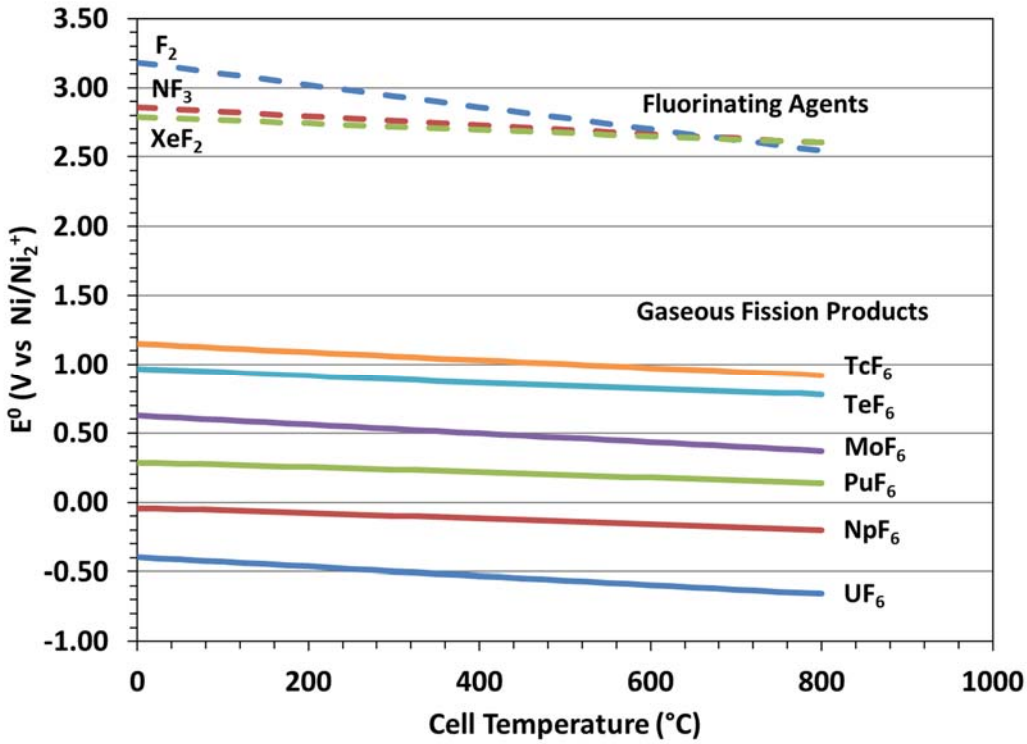

Figure 2: Calculations of reduction potentials for gaseous fission product formation from metallic elements relative to a Ni/NiF_2 reference electrode.

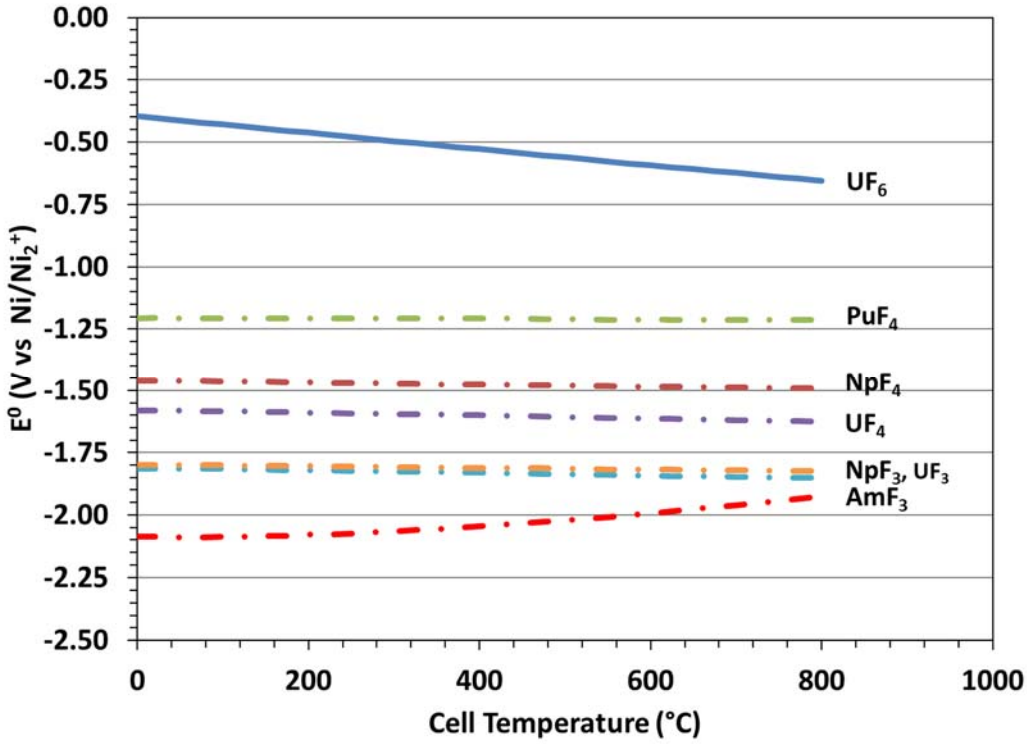

Figure 3: Calculation of uranium and TRU salt equilibrium potentials.

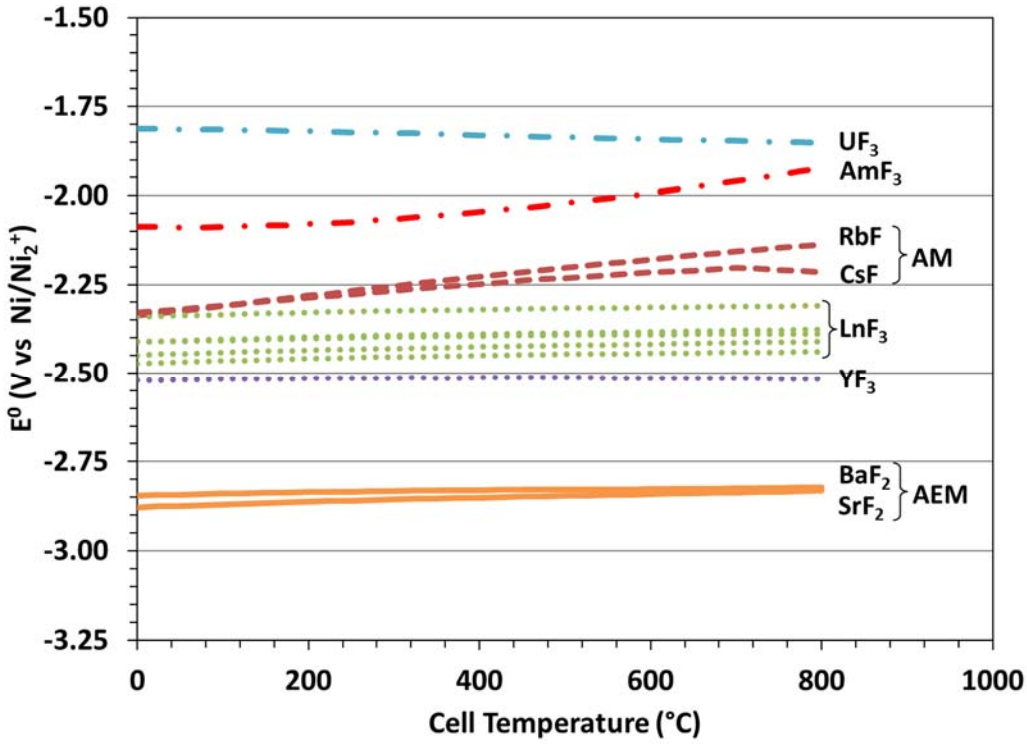

Figure 4: Calculation of AM, Ln, and AEM salt equilibrium potentials.

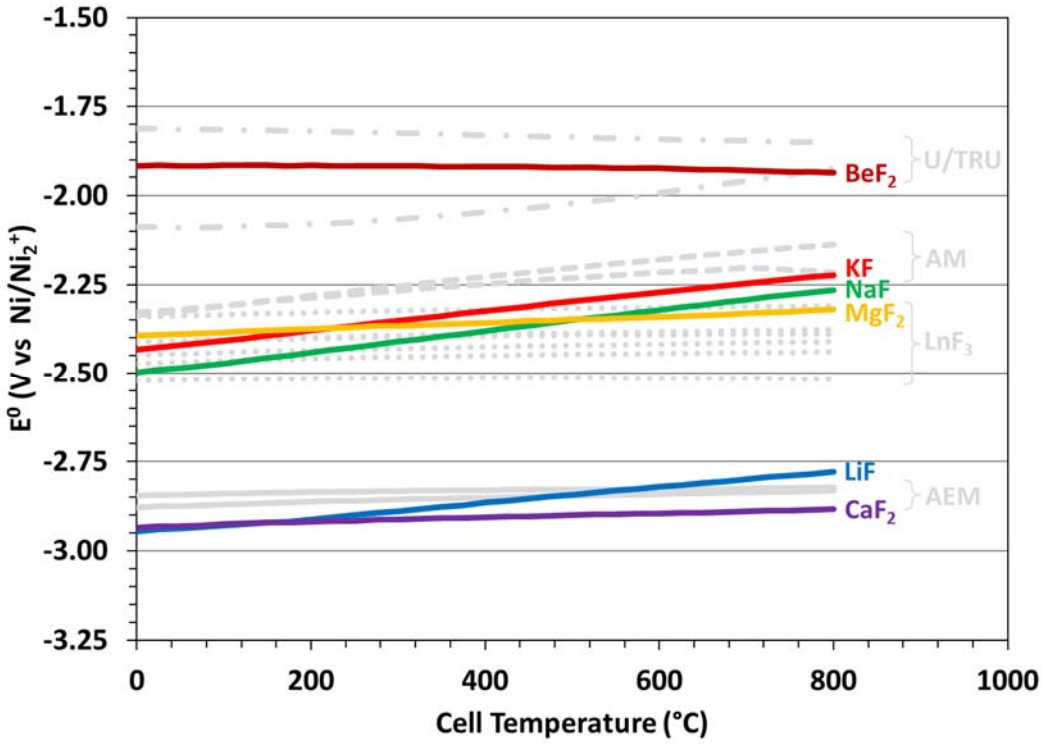

Figure 5: Calculation of potential molten salt constituent equilibrium potentials.

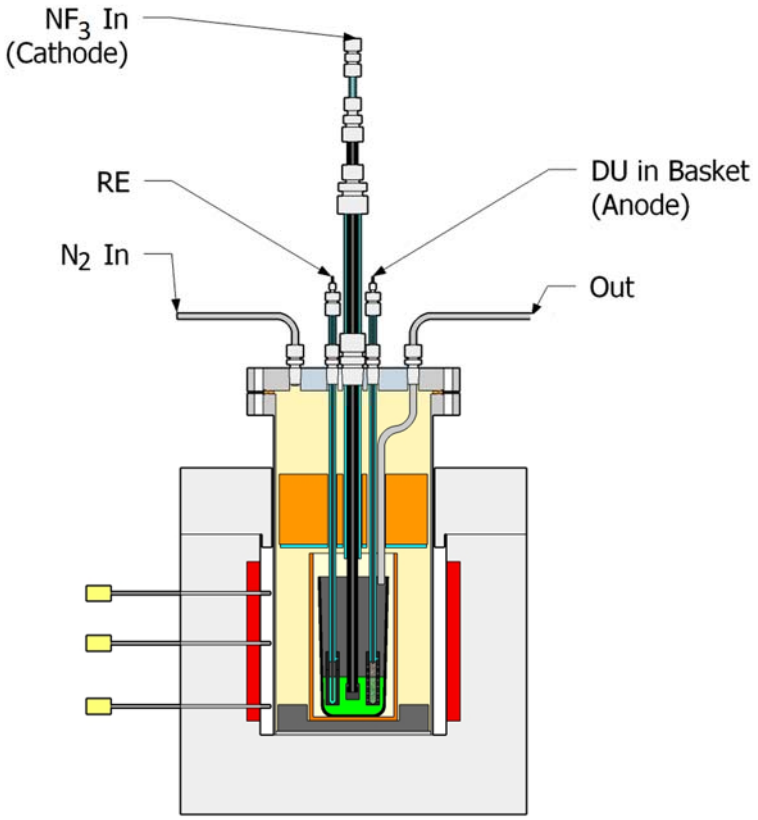

Figure 6: Schematic of electrochemical fluorination reactor. [23, 24]

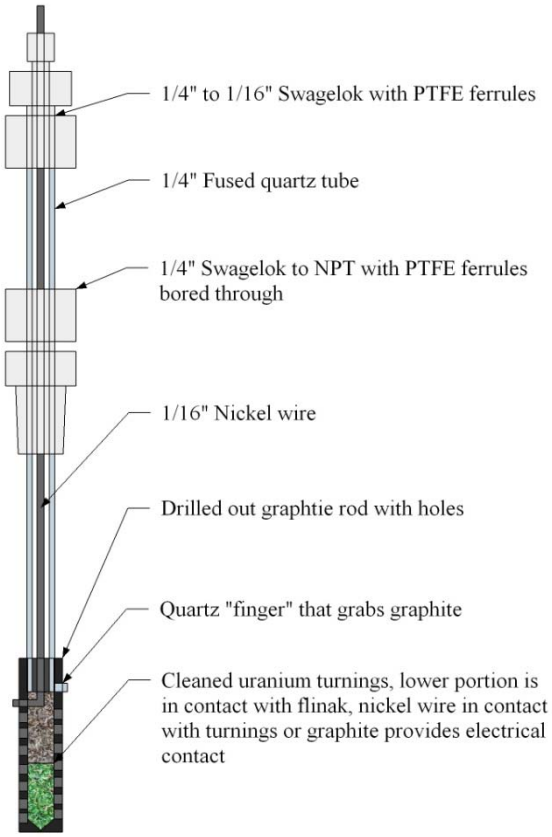

Figure 7: Schematic of anode for the electrochemical fluorination of DU.

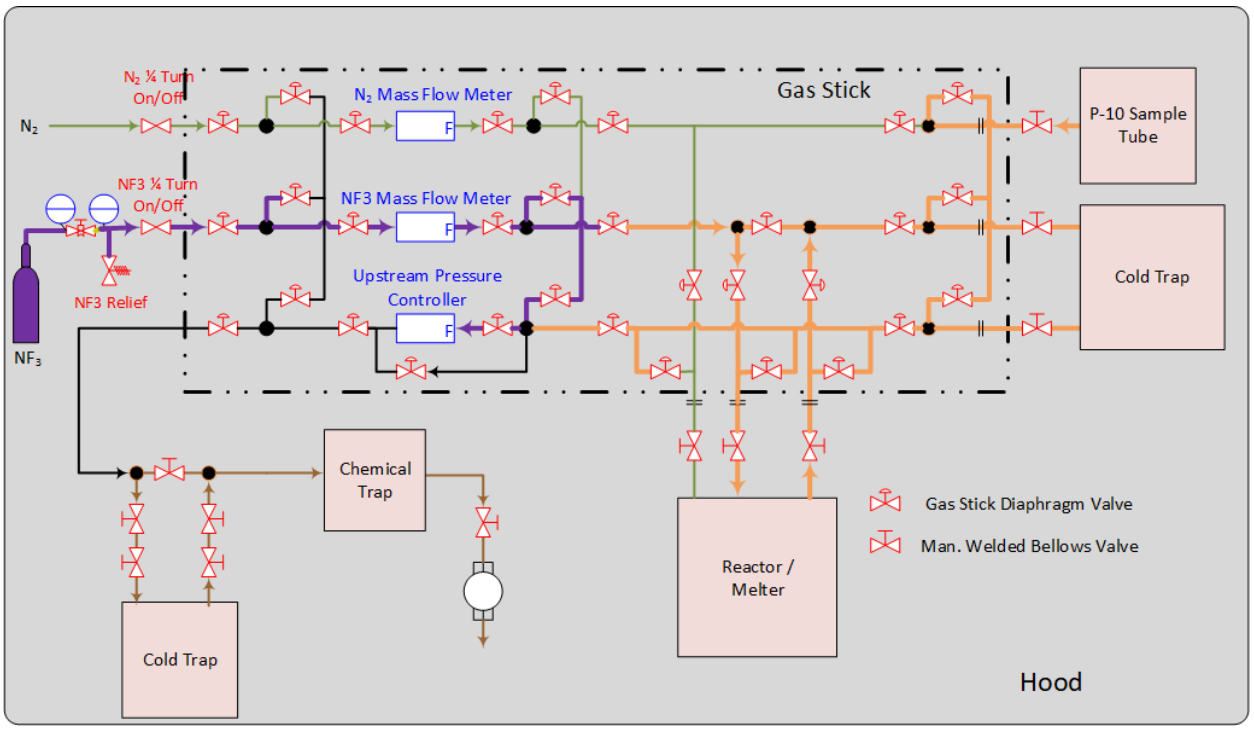

Figure 8: Flow diagram of electrochemical fluorination system.[23, 24]

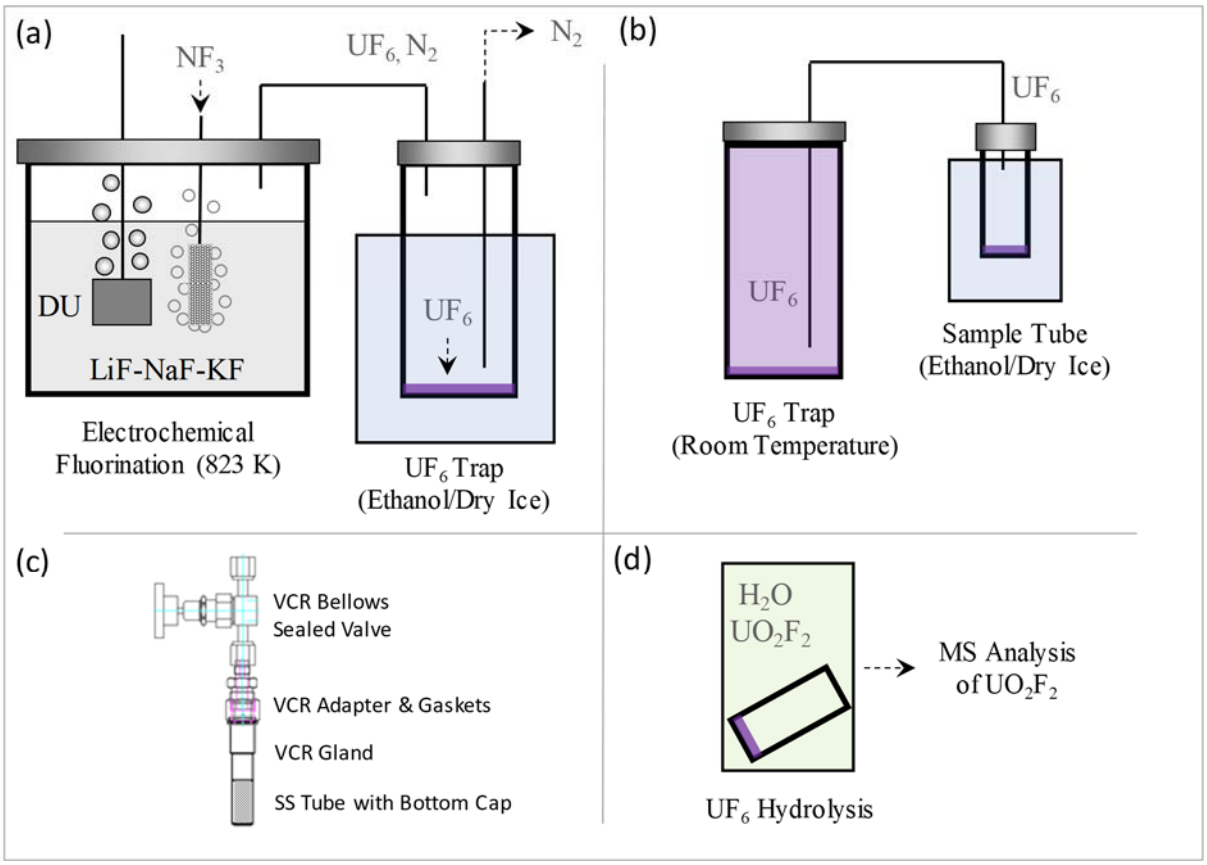

Figure 9: Schematic of EFS operation in (a) *reaction mode* and (b) *analysis preparation mode*. Also showing, schematic of (c) SCT for UF_6 collection and (d) hydrolysis for analysis of U.

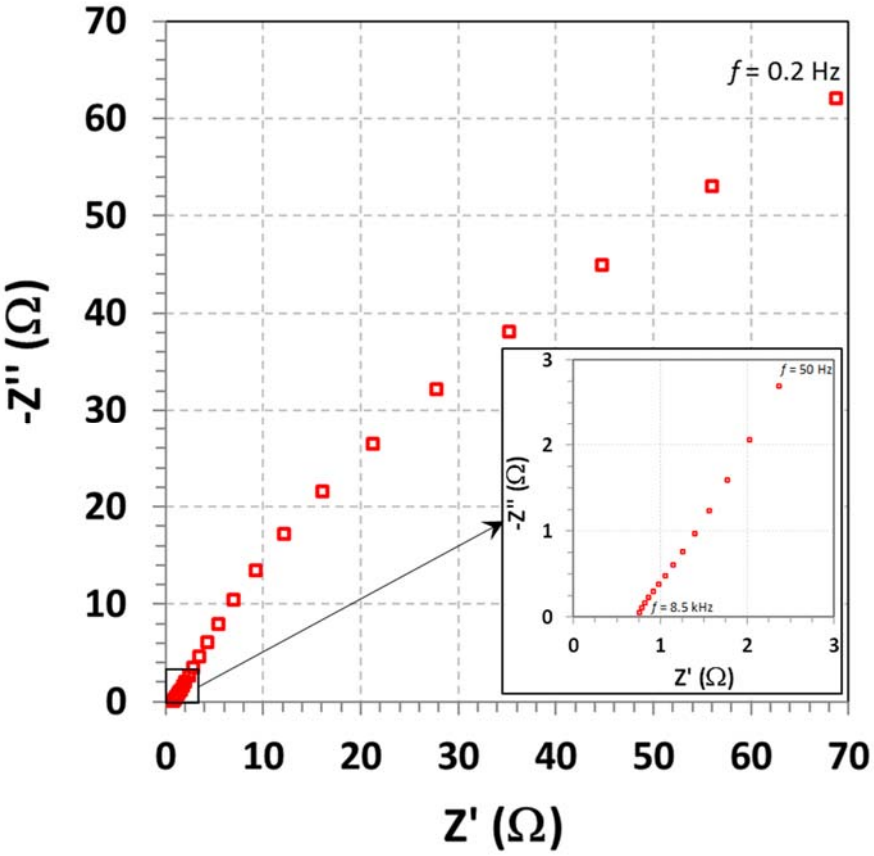

Figure 10: Nyquist plot for electrochemical cell under inert environment and at 550°C and 50 kPa before introducing NF_3.

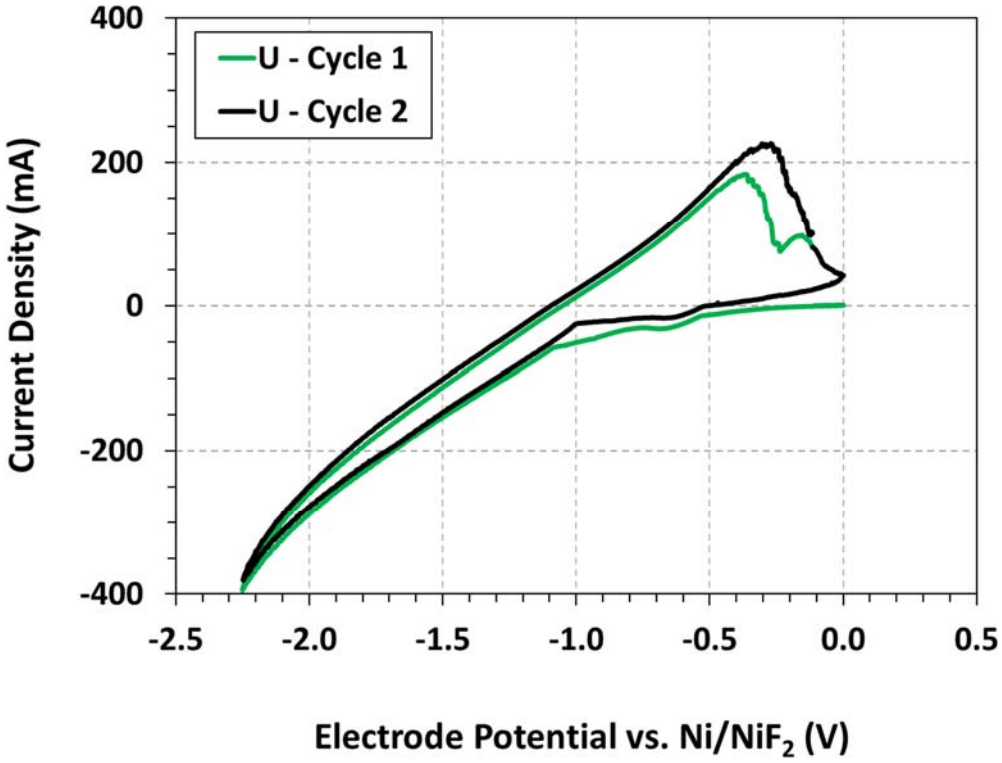

Figure 11: CV for electrochemical cell under inert environment at 550°C and 50 kPa before introducing NF_3.

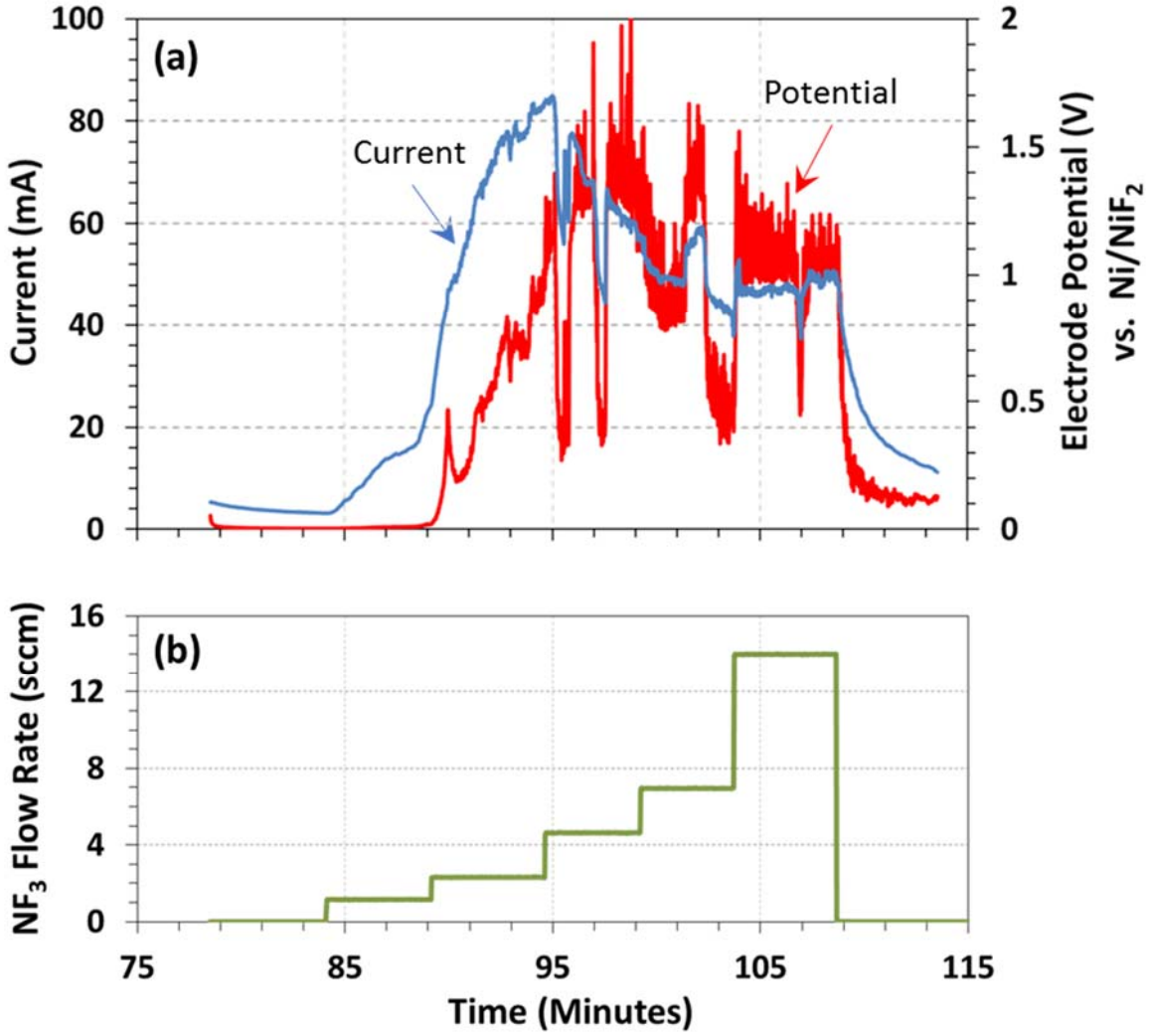

Figure 12: ZRA response for (a) current and working electrode potential as (b) NF_3 flow rate is introduced stepwise to the electrochemical cell at 550°C and 50 kPa.

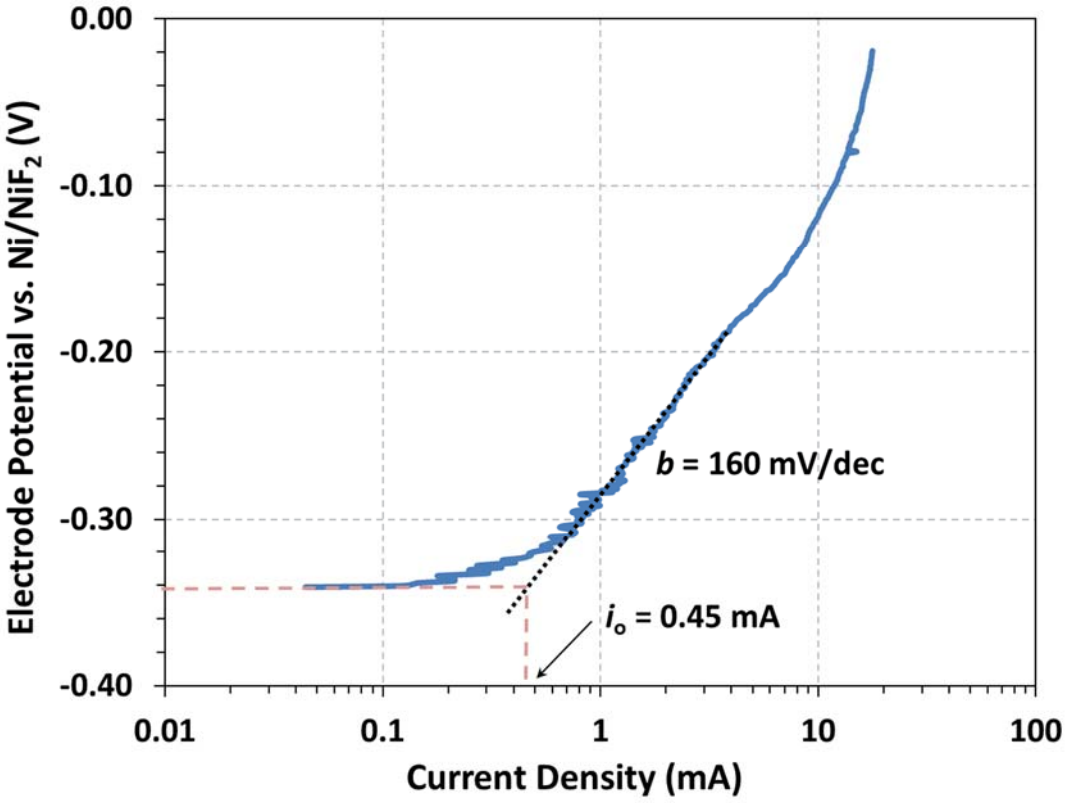

Figure 13: Polarization of electrochemical fluorination of U at 550°C and 50 kPa.

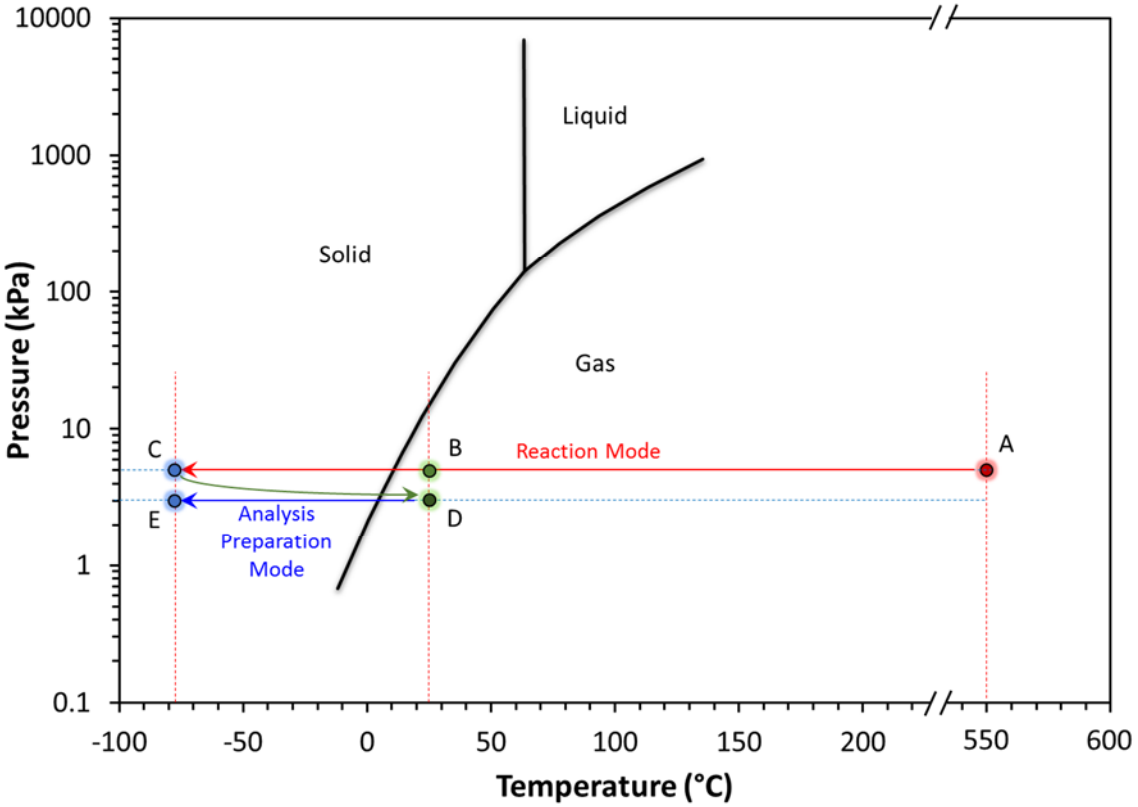

Figure 14: Phase diagram of UF_6 (data from Appendix A of the PEIS [31]) showing the conditions during the electrochemical fluorination and sample collection. In *reaction mode* UF_6 gas is produced in the reactor (A), move through the gas manifold (B) and desublime at the cold trap (C). A quick vacuum is applied to the cold trap and it is allowed to warm-up overnight (D). In *analysis preparation mode* UF_6 gas is transferred and desublimed at the SCT (E).